Research Article

The Most Unstable Conditions of Modulation Instability

Aifeng Tao,[1,2] Jinhai Zheng,[2,3] Soe Mee Mee,[4] and Botao Chen[2,3]

[1] *Key Laboratory of Coastal Disaster and Defence of Ministry of Education, Hohai University, Nanjing 210098, China*

[2] *College of Harbor, Coastal and Offshore Engineering, Hohai University, Nanjing 210098, China*

[3] *State Key Laboratory of Hydrology-Water Resources and Hydraulic Engineering, Hohai University, Nanjing 210098, China*

[4] *Department of Port & Harbour Engineering, Myanmar Maritime University, Yangon 11000, Myanmar*

Correspondence should be addressed to Jinhai Zheng, jhzheng@hhu.eud.cn

Modulation instability is one of the most ubiquitous types of instabilities in nature. As one of the key characteristics of modulation instability, the most unstable condition attracts lots of attention. The most unstable condition is investigated here with two kinds of initial wave systems via a numerical high-order spectral method (HOS) for surface water wave field. Classically, one carrier wave and a pair of sidebands are implied as the first kind of initial wave system: "seeded" wave system. In the second kind of initial wave system: "un-seeded" wave system, only one carrier wave is implied. Two impressive new results are present. One result shows that the grow rates of lower and upper sideband are different within the "seeded" wave system. It means that, for a given wave steepness, the most unstable lower sideband is not in pair with the most unstable upper sideband. Another result shows the fastest growing sidebands are exactly in pair from "unseeded" wave system. And the most unstable conditions of "unseeded" wave system are more or less the mean value of those derived from the lower sidebands and upper sidebands within the "seeded" wave system.

1. Introduction

As a typical nonlinear mechanism, the modulation instability (hereinafter referred as "MI"), also called Benjamin-Feir instability or self-modulation, has been observed and studied in numerous physical fields including water waves, plasma waves, laser beams, and electromagnetic transmission lines. As mentioned by Zakharov and Ostrovsky [1], there are between one and two million entries on MI in any internet search websites, for example,
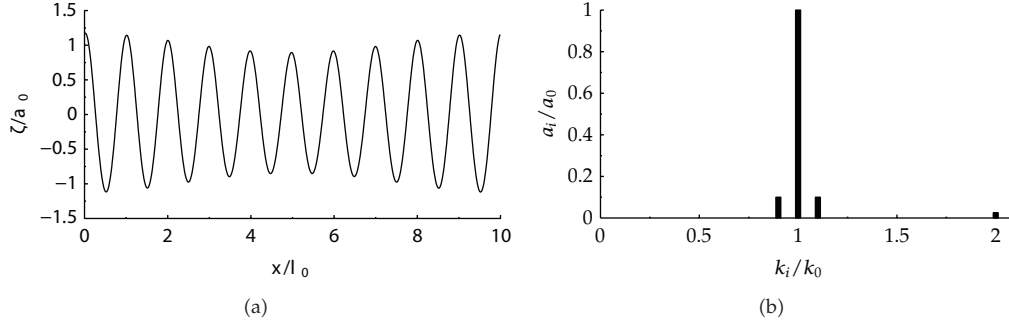
(a)

(b)

Figure 1: Sketch of initial surface elevation and wave number spectrum of Stokes modulated wave train for $\varepsilon_0 = 0.05$, $k_0 = 10$, $r_1 = 0.1$, $M = 4$, $N = 1024$, $T_0/\Delta t = 64$.

Yahoo. Even these references are not all equally relevant, the numbers are still enough to show the importance of MI. A recent usage of MI is to explain the possible reason for the occurrence of Freak waves [2], which may cause catastrophic damage to offshore structures and surface vessels due to exceptionally large amplitudes [3]. From this viewpoint, the Freak waves will appear at modulation peaks along the water wave evolution process. And it is well known that the water wave evolution process will reach the modulation peak within shortest time duration if the initial condition satisfies the most unstable condition (hereinafter referred as "MUC"). Generally, the MUC refers to the imposed wave train formed by a carrier wave and a pair of sidebands which will grow with the largest growth rate along the water wave evolution process. The latest comprehensive review and research work on MI we can refer to is Tulin and Waseda [4]. They reviewed nearly all the previous valuable works, including theoretical analysis, numerical simulation, and physical experiments. Particularly, based on a series delicate experiments, they explained the dynamic mechanisms of the sideband behavior in both the breaking and nonbreaking cases. The MUC they used in the experiments is calculated based on Krasitskii equation [5]. They mentioned that the results from Krasitskii equation are different with the previous results from Benjamin and Feir [6], Longuet-Higgins [7] and Dysthe [8]. But they did not discuss on that in details. The latest detailed experiments for MI were performed by Chiang [9] in a large wave tank (300 m long, 5.0 m wide, 5.2 m deep). The initial wave systems for his experiments are not only the imposed sidebands wave ("seeded") but also uniform wave ("un-seeded"). The initial uniform wave system has only the carrier wave. The sidebands will evolve and grow from background noises due to nonlinear wave interaction. As one of the Chiang's conclusions, the fastest growing modes of the naturally evolved sidebands in the experiments confirm the prediction of Tulin and Waseda [4] and that of Longuet-Higgins [7]. However, it is just roughly confirmed, especially for wave steepness less than 0.17. Due to physical experiment facility limitations, which include the tank length and the sidewall damping, the carrier wave steepness of all the previous experiments results is large than 0.1. However, the energetic wave steepness in the ocean is in the vicinity ($\varepsilon \sim 0.1$). Thus, it seems useful to do a detailed discussion on the determination of MUC.

In Section 2, the theoretical background of MI and the related modulated wave train are summarized. Section 3 introduces the research approach via numerical HOS method. The detailed numerical results are present in Section 4. And some discussions are listed in the last section.

2. Modulation Instability and Modulated Stoke Wave Train

Modulation instability (MI), can also be called Benjamin and Feir instability, was discovered by Lighthill [10], while it was proved analytically and validated experimentally by Benjamin and Feir [6]. The related milestone works have been reviewed by a lot of people, especially Tulin and Waseda [4], as already mentioned. Basically, a Stokes wave train is unstable to the perturbations or noises due to MI. Specifically, Benjamin and Feir [6] found that the unstable sideband components would grow exponentially with a time rate which depends on the dimensionless frequency difference between the carrier wave and unstable sideband and the initial wave steepness. Usually, the modulated Stokes wave train is defined by (2.1). As an example, the initial wave surface and the corresponding wave number spectrum are shown in Figure 1.

$$\varsigma(x,0) = \varsigma_0[\varepsilon_0, k_0] + r_- a_0 \cos(k_- x - \theta_-) + r_+ a_0 \cos(k_+ x - \theta_+),$$

$$\phi^s(x,0) = -\phi_0^s[\varepsilon_0, k_0] + \frac{r_-}{\sqrt{k_-}} a_0 e^{k_- \varsigma} \cos(k_- x - \theta_-) + \frac{r_+}{\sqrt{k_+}} a_0 e^{k_+ \varsigma} \cos(k_+ x - \theta_+). \tag{2.1}$$

Here, $\varsigma(x,0)$ and $\phi^s(x,0)$ are the surface elevation and surface potential at initial time $t = 0$. $\varsigma_0[\varepsilon_0, k_0]$ and $\phi_0^s[\varepsilon_0, k_0]$ are calculated for the carrier wave according to Schwartz [11] with respect to wave steepness ε_0 and wave number k_0. All the subscripts 0, +, − mentioned in this paper represent the carrier wave, upper sideband, and lower sideband, respectively. θ is the initial phase. It has been proved that the wave train evolution only vary with a phase combination $\theta' \equiv \theta_+ + \theta_- - 2\theta_0$. r is the ratio between the amplitudes of the sideband and carrier wave. As the detailed discussion by Tao [12], there are no fundamental different effects to the wave train evolution for different r_- and r_+. Then we define $r \equiv r_- = r_+$.

According to results of Benjamin and Feir, MI works only when (2.2) is satisfied.

$$r_1 < 2\sqrt{2}\varepsilon_0, \tag{2.2}$$

where $r_1 \equiv \Delta k / k_0$, $\Delta k \equiv k_+ - k_0 = k_0 - k_-$ and k is the wave number. For a given ε_0, there should be a corresponding r_1 which can induce the fastest sidebands growth and this can be called the most unstable condition (MUC), which is the emphasis of this paper. Including the choice of MUC, there are still some parameters for the modulated Stokes wave train that need to be determined, including the normalized carrier wave number (k_0), the nonlinear order of the carrier Stokes wave (M_s), the ratio (r) between the sidebands amplitudes and the carrier wave, and the initial phase (θ).

2.1. The Determination of k_0

The determination of k_0 is also related to numerical HOS method, which will be introduced in Section 3. In the calculation process of numerical HOS method, both the temporal and spatial parameters, including the wave numbers, have been normalized. Usually, the calculation domain is normalized to 2π. Then there would be 40 single harmonic waves present in the whole calculation domain 2π, if $k_0 = 40$, as shown in Figure 1. In order to keep enough precision for the depicture for the surface elevation in the physical domain, the number of wave modes N used in the numerical HOS method has to be large enough for large k_0, then
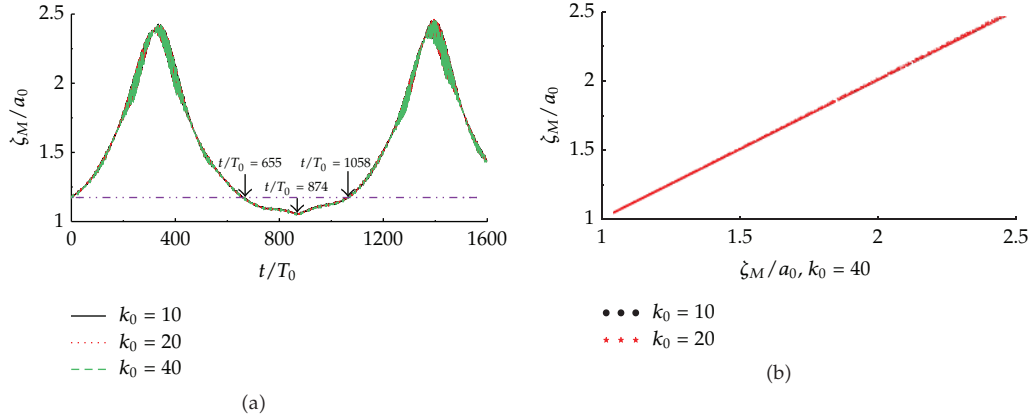
Figure 2: The maximum wave crest histories (a) and scatter diagram (b) of Stokes-modulated wave train for $\varepsilon_0 = 0.05$, $r_1 = 0.1$ with different $k_0 = 10$, 20 and 40.

the calculation time would increase. Fortunately, as discussed by Tao et al. [13], there is no essential difference for different k_0 with the same r_1, at least for time to $O(T_0 \varepsilon_0^{-3})$. In another word, for $\varepsilon_0 = 0.05$ with MUC ($r_1 = 0.1$), choosing $k_0 = 10$ and $\Delta k = 1$, $k_0 = 20$ and $\Delta k = 2$ or $k_0 = 40$ and $\Delta k = 4$, there would be exact no difference for investigation of the wave train evolution, as shown in Figure 2. In Figure 2 and the following paper, the maximum wave crest amplitude, denoted by ζ_M, is used frequently as a typical signal for the large wave. Due to this reason, the smallest k_0 is selected in this research only if it can allow the most unstable condition can be satisfied.

2.2. The Selection of M_s

Physically, the initial wave train, even a monochromatic Cosine wave, can be adjusted to nonlinear wave train by the nonlinear water wave equations within $O(T_0 \varepsilon_0^{-1})$. Dommermuth [14] has studied the adjustment process of numerical HOS method in details and he advised a considerable adjustment scheme in order to make the adjustment process smooth. To make sure the potential influence results from different initial carrier wave, four cases are performed here. As shown in the left picture of Figure 3, there are no fundamental differences for the dominant property of the wave train evolution. Although the carrier uniform cosine wave or lower Stokes wave do present the vibration phenomenon as shown in the right picture of Figure 3, there are nearly no difference if the order of carrier Stokes wave, denoted as M_s, is higher than 3. Then in all the following research cases, $M_s = 4$.

2.3. The Selection of the Amplitude Ratio r and Initial Phase θ

As mentioned by Tao [12], if r is small enough, with an experimental criterion being $r \times \varepsilon_0 < 0.02$, there would be no different effects to the sideband growth rate. Obviously, for a give carrier wave, larger r corresponds to large system energy, then the recurrence period is shorter and the maximum wave height is larger. Although it would be more relevant to lab freak wave generation, it is not the emphasis of this paper. A general value $r = r_- = r_+ = 0.1$ is employed in the whole research of this paper.
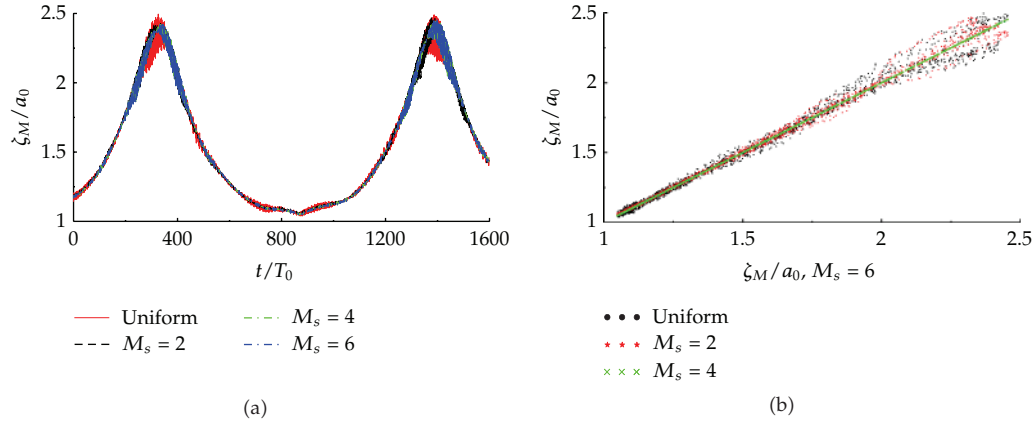
Figure 3: The maximum wave crest histories (a) and scatter diagram (b) of Stokes-modulated wave train for $\varepsilon_0 = 0.05$, $r_1 = 0.1$ with different initial carrier wave.

As one of the milestone works of modulation instability, Benjamin and Feir [6] showed that the initial phase corresponding to MUC is $\theta' \equiv \theta_+ + \theta_- - 2\theta_0 = 90°$. Based on a fully nonlinear irrational flow solver, Henderson et al. [15] mentioned that θ' would be some value between 15° and 35°. Tao [12] reinvestigated the effects of initial phase and deduced the same result in Benjamin and Feir [6]. This point will be of further research in another paper related to MUC determination. However, the initial phase is of no concern here, since it only takes action to the occurrence time for the first modulation peak and the recurrence period. There are no effects to the strength of the freak waves, which is the emphasis of this paper, as shown in Figure 4. Then it does make sense to choose any initial phase. Simply, we use $\theta_+ = \theta_- = 45°$ and $\theta_0 = 0°$.

3. High Order Spectra Method and Necessary Calibration Processes

The main research approach here is a high-order spectral method, which was developed by Dommermuth and Yue [16]. This method is capable of following nonlinear evolution of a large number of wave modes (N) with a minimum computation requirement. For convenience, we call this approach as HOS. The method includes nonlinear interactions of all wave components up to an arbitrary order (M) in wave steepness. The computational effort is almost linearly proportional to M and the large number of wave modes (N). Exponential convergence of the solution with M and N is also obtained. Unlike the phase-averaged and model-equation-based approaches, HOS accounts for physical phase-sensitive effects in a direct way. These include the initial distribution of wave phases in the wave-field specified by wave spectrum and energy dissipation due to wave breaking. The validity and efficacy of HOS have been established in the study of basic mechanisms of nonlinear wave-wave interactions in the presence of atmospheric forcing [17], long-short waves [18], finite depth and depth variations [19], submerged/floating bodies [20], and viscous dissipation [21].

The feasibility of HOS to reveal the characteristics of MI has been fully proved by Dommermuth and Yue [16]. While the determination of some key parameters, including the nonlinear wave order M, the wave modes number N and the numerical integral time step Δt still need to be discussed in details.
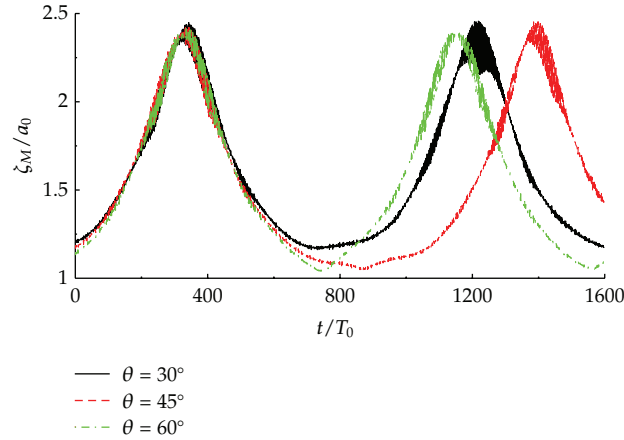
Figure 4: The maximum wave crest histories of Stokes modulated wave train for $\varepsilon_0 = 0.05$, $r_1 = 0.1$ with different initial phases.

A general approach for the determination of M, N, and Δt has been provided by Dommermuth and Yue [16] for practical computations. For a desired accuracy δ, M can be chosen to satisfy $\delta = \varepsilon^M$. For example, $M = 4$ can reach the accuracy $\delta = 10^{-4}$ for $\varepsilon = 0.05$ to 0.07. N and Δt can be got from the two tables provided by Dommermuth and Yue [16]. Based on this approach, ten numerical cases are performed to determine the suitable M, N, and Δt for this research. As shown in Figure 5, $M = 2$ cannot capture the physical evolution process, while the results of $M = 3$ and 4 are almost the same. Considering the accuracy, $M = 4$ is employed here. From Figure 6, it can be seen clearly that all of these three cases can be used. $N = 1024$ is selected here. All the chosen values of dt can satisfy the Courant condition $\Delta t^2 \leqslant 8\Delta x/\pi$; however, the precision depends on the evolution time, as shown in Figure 7. $T_0/\Delta t = 64$ is employed here.

4. Numerical Experiments and Results

In order to investigate the detailed information of MUC, two kinds of numerical experiments are performed based on HOS. The first kind of initial wave system, hereinafter calling it "seeded" wave system, is formed by a carrier wave and a pair of sidebands. This corresponds to the imposed or "seeded" wave system in physical experiments. The second kind of initial wave system, hereinafter calling it "un-seeded" wave system, has only a carrier wave, while this carrier wave is calculated based on Stokes wave theory. This is similar to the uniform or "un-seeded" wave system in physical experiments. For the "un-seeded" wave system, the background noises in the tank are mainly from the multiple reflections of the wave front, while those noises in the numerical experiments are from computer round of errors. Because there are no pure zero can be gotten from the computer. Even using the double-precision floating-point format, the zero is still stored as ~10^{-16}, as shown in Figure 8, which is the Fourier spectra of a "un-seeded" initial wave train for case $\varepsilon_0 = 0.05$. To show the background noise, the vertical Log coordinate is used.

Based on the preliminary works listed in Sections 2 and 3 , some common parameters are selected for both kinds of initial wave systems listed in Table 1. There are nine cases
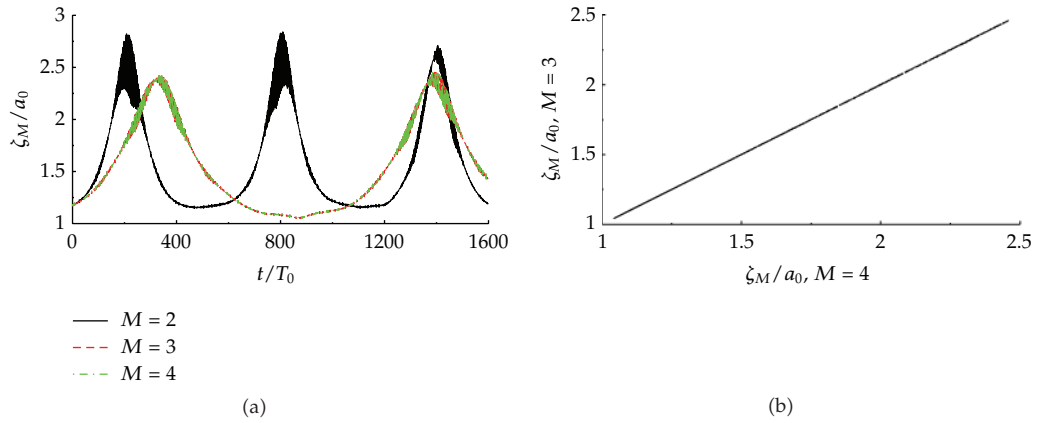
(a)

(b)

Figure 5: The maximum wave crest histories (a) and scatter diagram (b) of Stokes-modulated wave train for $\varepsilon_0 = 0.05$, $r_1 = 0.1$, $N = 1024$, $T_0/\Delta t = 64$ with different M.
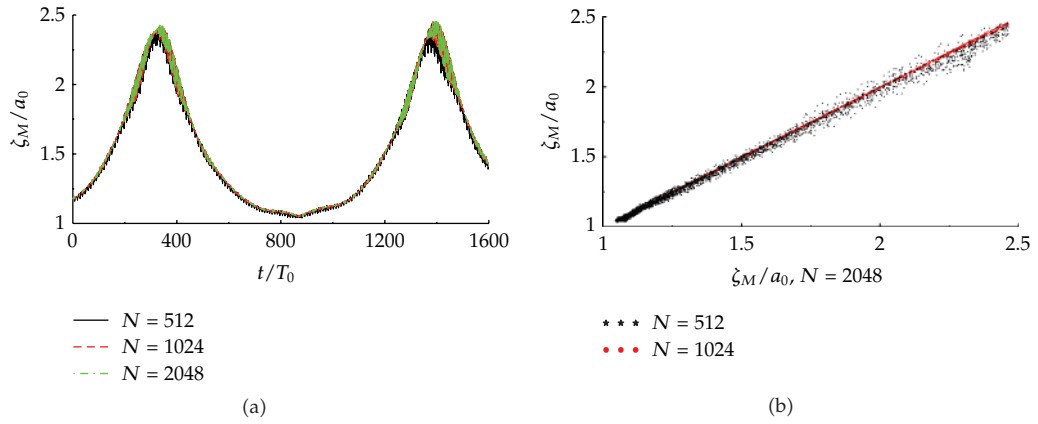

(a)

(b)

Figure 6: The maximum wave crest histories (a) and scatter diagram (b) of Stokes-modulated wave train for $\varepsilon_0 = 0.05$, $r_1 = 0.1$, $M = 4$, $T_0/\Delta t = 64$ with different N.
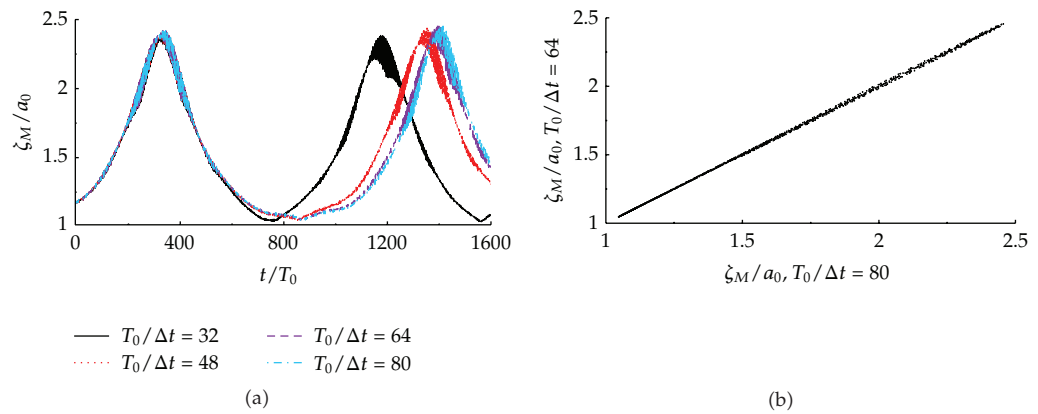

(a)

(b)

Figure 7: The maximum wave crest histories (a) and scatter diagram (b) of Stokes-modulated wave train for $\varepsilon_0 = 0.05$, $r_1 = 0.1$, $M = 4$, $N = 1024$ with different Δt.

Table 1: Common parameters for both kinds of numerical experiments.

k_0	M_s	M	N	$T/\Delta t$
100	4	4	1024	64

Table 2: Parameters $\Delta k/k_0$ for initial imposed wave system.

ε_0	r_1	ε_0	r_1
0.05	$0.04, 0.05, \ldots, 0.13$	0.10	$0.14, 0.15, \ldots, 0.23$
0.06	$0.06, 0.07, \ldots, 0.15$	0.12	$0.18, 0.19, \ldots, 0.27$
0.07	$0.08, 0.09, \ldots, 0.17$	0.14	$0.22, 0.23, \ldots, 0.31$
0.08	$0.10, 0.11, \ldots, 0.19$	0.16	$0.26, 0.27, \ldots, 0.35$
0.09	$0.12, 0.13, \ldots, 0.21$		

selected for both kinds. Each case is given a different carrier wave steepness, ε_0 = 0.05, 0.06~0.10, 0.12, 0.14, 0.16.

Each "seeded" wave train evolution, with specific carrier wave steepness, is simulated with ten different sideband pairs to the first modulation peak. The related parameters r_1 and $\Delta k/k_0$ are listed in Table 2. In addition, the initial phases are selected as $\theta_+ = \theta_- = 45°$ and $\theta_0 = 0°$. The amplitude ratio between sidebands and carrier wave are selected as $r_- = r_+ = 0.1$ at $t = 0$. In all realizations, the k_0 selected as 100. Generally, the growth rates of sidebands need to be calculated and compared in order to get the fastest growing sideband. Here the growth rate β satisfies:

$$r_\pm\left(\tilde{t}\right) = r_\pm(t = 0) \exp\left(\beta\tilde{t}\right), \tag{4.1}$$

where the $\tilde{t} = \omega t$ and ω used in this research is the angular frequency of carrier wave. This formula is transformed simply from the common space domain version. However, we find that the growth rate is not so clear to show which sideband is faster, since it is not pure steady with the time varying, even just for the initial stage. For an example, we list the varying growth rate of lower and upper sideband for case $\varepsilon_0 = 0.05$ with $\Delta k/k_0 = 0.09$ in Table 3. It is difficult to select the suitable time duration. So, instead of calculating the sidebands growth rates, the amplitude evolution processes for all the lower sidebands and upper sidebands are plotted together, respectively, for each case. Then the fastest growing sideband can be easily seen. For instance, we plot in Figure 9 the evolution processes of all the lower sidebands for case $\varepsilon_0 = 0.06$ before the first modulation peak. In order to make the picture clearer, only the sidebands close to the fastest one are showed. Obviously, the fastest growing sideband can be captured directly. Particularly, Figure 9 reveals that the fastest growing lower sideband corresponds to $r_1 = 0.1$, while the fastest growing upper sideband corresponds to $r_1 = 0.11$. It is not in pair. According to this procedure, we can get the fastest growing sidebands for all the cases. The results together with typical previous results are plotted in Figure 10. In this figure, "Dysthe 1979" is the result calculated by Dysthe based on a modified Nonlinear Schrödinger equation [8]. "Tulin and Waseda 1999" refers to the results calculated by Tulin and Waseda [4] based on Krasitskii equation. "Benjamin and Feir 1967" is the result calculated by Benjamin and Feir [6] based on the classical third-order Nonlinear Schrödinger equation. "Chiang 2005" is the experiment results given by Chiang [9]. "Lower from seeded" and "Upper from seeded" are the results from this research. The former one is the MUC based on

Table 3: The growth rates varying with time for case $\varepsilon_0 = 0.05$ with $r_1 = 0.09$.

Time	Modulation peak	300	295	290–115	110	100	95	80	60	40
Lower	0.08	0.08	0.08	0.09	0.08	0.08	0.08	0.08	0.04	0.04
Upper			0.09				0.08	0.08	0.07	0.04
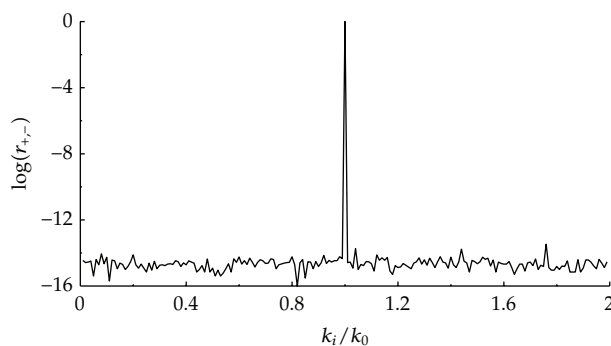
Figure 8: The Fourier spectra of the "un-seeded" initial wave system for case $\varepsilon_0 = 0.05$.

the comparison of lower sidebands. And the latter one is based on the comparison of upper sidebands. Clearly, the "Upper from seeded" matches both the theoretical result of Tulin and the experimental result of Chiang.

For the "un-seeded" wave system, the fastest growing sidebands can be captured straightforwardly. For an example, we plot the evolution processes of all the "naturally" evolving sidebands for case $\varepsilon_0 = 0.06$ in Figure 11. It is quite easy to assure the fastest growing sideband is $r_1 = 0.11$. Unlike the result from "seeded" wave system, the fastest growing lower sideband is in pair with the upper sideband perfectly for all the nine cases. The final results are also plotted in Figure 10 in order to make a detailed comparison. From Figure 10, it is easy to conclude that the fastest growing sidebands from "un-seeded" wave system are more like the mean of that of the lower and upper sideband from "seeded" wave system.

5. Conclusions

Focusing the determination of the most unstable conditions for modulation instability, a series of numerical experiments were designed and performed via a robust phase-resolved numerical model HOS for the surface water wave field. The key points of this paper can be divided into three parts. The first is the detailed discussion for the parameters of both MI and HOS, such as the normalized carrier wave number (k_0). The second is the numerical experiment design. In order to make a comprehensive comparison with previous works, both the "seeded" and "un-seeded" initial wave systems are investigated. The third, and also the main contribution, is that we find two new results. One result shows that the grow rates of lower and upper sideband are different even at the very initial stage. It means that, for a given wave steepness, the most unstable lower sideband is not exactly in pair with the most unstable upper sideband. And the most unstable conditions derived from upper sidebands are more close to the previous results, including both the numerical and experimental results. Another result shows that the fastest growing sidebands are exactly in pair for the "un-seeded" wave system. And the most unstable conditions of "un-seeded" wave system are
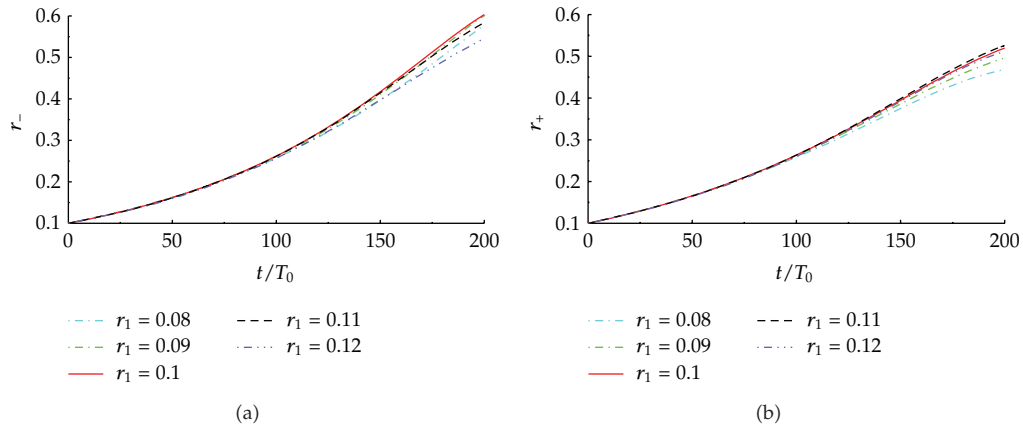
(a)   (b)

Figure 9: The amplitude evolution processes of lower sidebands (a) and upper sidebands (b) for case $\varepsilon_0 = 0.06$.

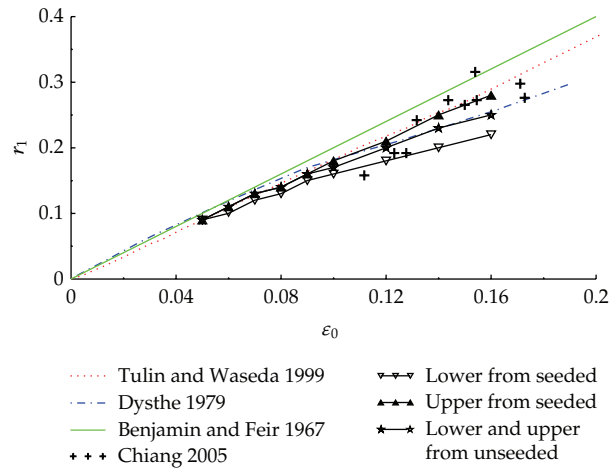**Figure 10:** The MUC for different carrier wave steepness.

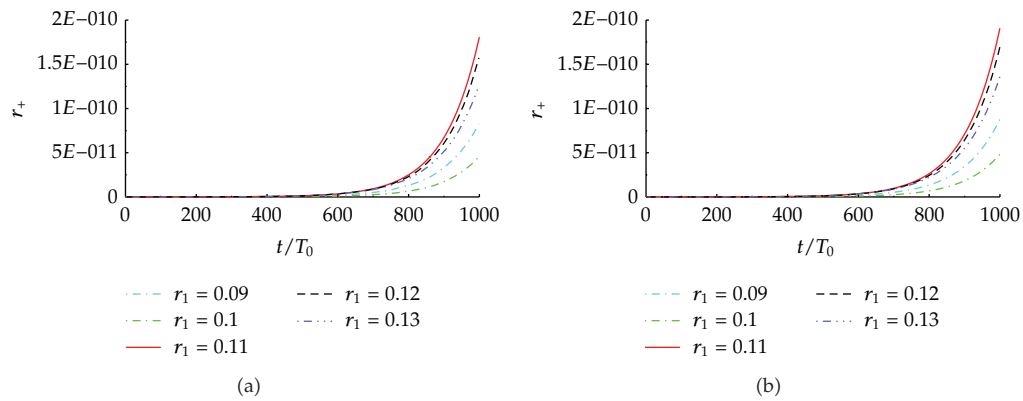(a)   (b)

Figure 11: The sideband evolution processes from the background noise for "un-seeded" wave system with case $\varepsilon_0 = 0.06$.

more or less the mean value of those derived from the lower sidebands and upper sidebands within the "seeded" wave system. For a suitable explanation of these results further detailed research is needed.

Acknowledgments

References

[1] V. E. Zakharov and L. A. Ostrovsky, "Modulation instability: the beginning," *Physica D*, vol. 238, no. 5, pp. 540–548, 2009.

[2] V. E. Zakharov, A. I. Dyachenko, and A. O. Prokofiev, "Freak waves as nonlinear stage of Stokes wave modulation instability," *European Journal of Mechanics B*, vol. 25, no. 5, pp. 677–692, 2006.

[3] G. Lawton, "Monsters of the deep," *New Scientist*, vol. 170, no. 2297, pp. 28–32, 2001.

[4] M. P. Tulin and T. Waseda, "Laboratory observations of wave group evolution, including breaking effects," *Journal of Fluid Mechanics*, vol. 378, pp. 197–232, 1999.

[5] V. P. Krasitskii, "On reduced equations in the Hamiltonian theory of weakly nonlinear surface waves," *Journal of Fluid Mechanics*, vol. 272, pp. 1–20, 1994.

[6] T. B. Benjamin and J. E. Feir, "The disintegration of wave trains on deep water, part I. Theory," *Journal of Fluid Mechanics*, vol. 27, pp. 417–430, 1967.

[7] M. S. Longuet-Higgins, "Modulation of the amplitude of steep wind waves," *Journal of Fluid Mechanics*, vol. 99, no. 4, pp. 705–713, 1980.

[8] K. B. Dysthe, "Note on a modication to the nonlinear Schrödinger equation for application to deep water waves," *Proceedings of the Royal Society of London A*, vol. 369, pp. 105–114, 1979.

[9] W. S. Chiang, *A study on modulation of nonlinear wave trains in deep water*, Ph.D. thesis, National Cheng-Kung University, Taiwan,China, 2005.

[10] M. J. Lighthill, "Contributions to the theory of waves in non-linear dispersive systems," *IMA Journal of Applied Mathematics*, vol. 1, no. 3, pp. 269–306, 1965.

[11] L. W. Schwartz, "Computer extension and analytic continuation of Stokes expansion for gravity waves," *Journal of Fluid Mechanics*, vol. 62, no. 3, pp. 553–578, 1974.

[12] A. F. Tao, *Nonlinear wave trains evolution and freak wave generation mechanisms in deep water*, Ph.D. thesis, Hohai University, Nanjing, China, 2007.

[13] A. F. Tao, J. H. Zheng, S. Mee Mee, and B. T. Chen, "Re-study on recurrence period of stokes wave train with high order spectral method," *China Ocean Engineering*, vol. 25, no. 3, pp. 679–686, 2011.

[14] D. G. Dommermuth, "The initialization of nonlinear waves using an adjustment scheme," *Wave Motion*, vol. 32, no. 4, pp. 307–317, 2000.

[15] K. L. Henderson, D. H. Peregrine, and J. W. Dold, "Unsteady water wave modulations: fully nonlinear solutions and comparison with the nonlinear Schrödinger equation," *Wave Motion*, vol. 29, no. 4, pp. 341–361, 1999.

[16] D. G. Dommermuth and D. K. P. Yue, "A high-order spectral method for the study of nonlinear gravity waves," *Journal of Fluid Mechanics*, vol. 184, pp. 267–288, 1987.

[17] D. G. Dommermuth and D. K. P. Yue, "The nonlinear three-dimensional waves generated by a moving surface disturbance," in *Proceedings of the 17th Symposium on Naval Hydrodynamics*, pp. 59–71, National Academy Press, Hague, The Netherlands, 1988.

[18] J. Zhang, K. Hong, and D. K. P. Yue, "Effects of wavelength ratio on wave modelling," *Journal of Fluid Mechanics*, vol. 248, pp. 107–127, 1993.

[19] Y. M. Liu and D. K. P. Yue, "On generalized Bragg scattering of surface waves by bottom ripples," *Journal of Fluid Mechanics*, vol. 356, pp. 297–326, 1998.

[20] Y. M. Liu, D. G. Dommermuth, and D. K. P. Yue, "A high-order spectral method for nonlinear wave-body interactions," *Journal of Fluid Mechanics*, vol. 245, pp. 115–136, 1992.

[21] G. Y. Wu, Y. M. Liu, and D. K. P. Yue, "A note on stabilizing the Benjamin-Feir instability," *Journal of Fluid Mechanics*, vol. 556, pp. 45–54, 2006.